



Associations of brain entropy (BEN) to cerebral blood flow and fractional amplitude of low-frequency fluctuations in the resting brain

Donghui Song¹ · Da Chang¹ · Jian Zhang¹ · Qiu Ge¹ · Yu-Feng Zang¹ · Ze Wang^{1,2} 

Published online: 12 September 2018
© Springer Science+Business Media, LLC, part of Springer Nature 2018

Abstract

Entropy is a fundamental trait of human brain. Using fMRI-based brain entropy (BEN) mapping, interesting findings have been increasingly revealed in normal brain and neuropsychiatric disorders. As BEN is still relatively new, an often-raised question is how much new information can this measure tell about the brain compared to other more established brain activity measures. The study aimed to address that question by examining the relationship between BEN and cerebral blood flow (CBF) and the fractional amplitude of low-frequency fluctuations (fALFF), two widely used resting state brain state measures. fMRI data acquired from a large cohort of normal subjects were used to calculate the three metrics; inter-modality associations were assessed at each voxel through the Pearson correlation analysis. A moderate to high positive BEN-CBF and BEN-fALFF correlations were found in orbito-frontal cortex (OFC) and posterior inferior temporal cortex (ITC); Strong negative BEN-fALFF correlations were found in visual cortex (VC), anterior ITC, striatum, motor network, precuneus, and lateral parietal cortex. Positive CBF-fALFF correlations were found in medial OFC (MOFC), medial prefrontal cortex (MPFC), left angular gyrus, and left precuneus. Significant gender effects were observed for all three metrics and their correlations. Our data clearly demonstrated that BEN provides unique information that cannot be revealed by CBF and fALFF.

Keywords Brain entropy · Resting state fMRI · Cerebral blood flow · Fractional amplitude of the low-frequency fluctuations

Introduction

Entropy is a physical measure for system irregularity or uncertainty with high entropy meaning high irregularity or disorder (Clausius 1862; Singer 2009). Human brain is a complex dynamic system, which acts through its time-varying temporal activity. Entropy of brain activity, which is equivalent to information according to Shannon's information theory (Shannon 1948), indicates the capability of the brain for processing either incoming or outgoing information. High temporal brain Entropy (BEN) often represents a beneficial trait of human brain, which might have played a fundamental

evolutional role for the human beings to better recognize threats and opportunities to survive in the constantly changing environment (Macphail and Bolhuis 2001; Roth and Dicke 2012; Hofman 2014; Rilling 2014). Entropy is also related to complexity though they diverge after complexity reaches the peak (Tononi et al. 1998; Goldberger et al. 2002; Lipsitz 2004; Singer 2009). Because of the difficulty of defining a complexity measure, many studies are still using entropy to approximately indicate complexity (Richman and Moorman 2000; Lake et al. 2002). In the human brain, most studies concluded a high complexity during its normal state but a loss of complexity during diseased condition (Friston et al. 1992; Tononi et al. 1998; Goldberger et al. 2002; Lipsitz 2004; Singer 2009; Friston et al. 2010; Bassett and Gazzaniga 2011). Nevertheless, we would stick to the nomenclature of entropy to keep the descriptions less confusion.

BEN has long been assessed using electrophysiological data (Mölle et al. 1996; Bhattacharya 2000; Richman and Moorman 2000; Sabeti et al. 2009; Bosl et al. 2011), which often only provides one global value and lacks spatial resolution. A recent increasing research interest is

✉ Ze Wang
zewangnew@temple.edu

¹ Center for Cognition and Brain Disorders, Department of Psychology, Hangzhou Normal University, Hangzhou, China

² Department of Radiology, Lewis Katz School of Medicine, Temple University, 3401 N Broad Street, 1st Floor, Radiology, Philadelphia, PA 19140, USA

to map BEN using functional MRI (fMRI) (Yao et al. 2013; Smith et al. 2014; Lebedev et al. 2016; Li et al. 2016; Zhou et al. 2016; Jia et al. 2017; Nelson et al. 2017; Wang et al. 2017). In (Wang et al. 2014), we implemented an fMRI-based whole-brain entropy mapping algorithm and tool and applied it to a large size resting-state fMRI data ($n=1049$) to examine BEN distribution patterns in normal healthy brain. Subsequently, we applied the BEN mapping tool to a few brain diseases and identified disease-related alterations in multiple sclerosis (Zhou et al. 2016), chronic cigarette smoking (Li et al. 2016), and cocaine addiction (Ze Wang et al. 2017). More recently, we demonstrated that temporal BEN in the resting brain can be modulated by caffeine ingestion (Da et al. 2018) and local repetitive transcranial magnetic stimulation (Song et al. 2018). Along with BEN alterations identified by other groups in normal aging (Yang et al. 2013), schizophrenia (Sokunbi et al. 2014b), and attention deficit hyperactivity disorder (ADHD) (Sokunbi et al. 2014a), these findings clearly demonstrated the potential of BEN mapping in brain functionality studies in normal brain as well as in diseased conditions.

As BEN is still relatively new to the literature, an often-raised question is how much new information it can provide as compared to other more widely used brain activity measures. The purpose of this study is to address this open question with a large sample data. More specifically, we will consider the possible correlations of BEN to two others widely used brain measures: cerebral blood flow (CBF) and the fractional amplitude of low-frequency fluctuations (fALFF), two widely used resting state brain state measures (Fransson 2005; Zou et al. 2009; Lee et al. 2013). CBF is a physiological measure fundamental because of its tight to regional brain function due to the coupling to brain metabolism (Baron et al. 1982; Furlow Jr et al. 1983; DeWitt et al. 1988; Raichle 1998; Liu et al. 2004; Vestergaard et al. 2016). fALFF reflects the regional slow-wave brain activity strength and is empirically defined as the ration of the power within the low-frequency range (0.01–0.08 Hz) to the total power of the entire detectable frequency range (Zou et al. 2008). Because BEN is derived from the dynamic brain activity, which is not necessarily related to the baseline brain metabolism as indicated by CBF, we hypothesized that BEN is correlated to CBF only in a small portion of the brain cortices. While there is no definitive correlation between BEN and fALFF because BEN is a statistical measure but fALFF is a relative power spectrum measure of the low frequency signal component, low frequency signal often contributes less irregularity and therefore less entropy than high-frequency signal. Accordingly, we expected to see negative BEN-fALFF correlations in the resting brain in region exhibiting strong low-wave resting brain activity but no BEN-fALFF correlation in the rest of brain.

Methods

Participants

107 healthy participants (age: 31.49 ± 13.97 years, 49 males, 58 females) were recruited. All participants were right-handed and reported no history of neurological or psychiatric disorders. They were asked not drink any caffeinated beverages 12 h before the scan time. All study procedures adhered to the Declaration of Helsinki were approved by local IRB and all participants signed written consent forms before participating in any experiment in the study.

MRI data acquisition

All MR images were acquired with a 3 T Discovery MR 750 scanner (General Electric, Waukesha, WI, USA) at the Center for Cognition and Brain Disorders at Hangzhou Normal University, China. During the scan, a comfortable and tight cushion was placed to immobilize the head and reduce motion. The participants were instructed to relax and remain still with their eyes open, not to fall asleep, and not to think about anything in particular. Monitored through the video camera in the scanner room and no subjects were found to fall asleep during the scan, which was further confirmed by interview after the scan.

High-resolution T1-weighted structural MRI was acquired with a 3D spoiled gradient echo sequence (3D SPGR) with repetition time/echo time (TR/TE)=8.1/3.39 ms, flip angle = 7° , field of view = 256×256 mm², matrix = 256×256 , slice thickness = 1 mm, number of slices = 176, no gap between adjacent slices. Resting state blood-oxygen-level-dependent (BOLD) fMRI was measured with a T2*-weighted gradient-echo-planar imaging (EPI) pulse sequence with the following parameters: TR/TE = 2000/30 ms, flip angle = 90° , field of view = 220×220 mm², matrix = 64×64 , slice thickness = 3.4 mm, and 37 interleaved slices with no gap in between. 240 images were acquired in 8 mins.

The commercial 3D pseudo-continuous arterial spin labeling (ASL) perfusion MRI sequence from GE was used to acquire whole-brain CBF images. The sequence utilized a pseudo-continuous labeling technique and fast spin echo acquisition with interleaved stack of spiral readout and centric ordering in the slice-encoding direction. Background suppression consisted of a presaturation, four optimally timed inversion pulses for background tissue intensity suppression, and one inferior saturation pulse for suppressing signal from late incoming blood after spin labeling. Labeling time was

1450 ms. Post-label delay time was 1520 ms. TR/TE = 4690 ms/10.86 ms. Other sequence parameters were: slice thickness = 4 mm, in-plane resolution = $3.7 \times 3.7 \text{ mm}^2$, eight spiral interleaves, number of repetitions = 4 mm. In addition, a reference proton density weighted image was acquired for CBF quantification based on ASL signal. The entire ASL acquisition took approximately 8 min 34 s.

MRI image preprocessing

MR image preprocessing was performed using Statistical Parametric Mapping (SPM12, WELLCOMETRUST CENTRE FOR NEUROIMAGING, London, UK, <http://www.fil.ion.ucl.ac.uk/spm/software/spm12/>). Structural MRI was registered into the Montreal Neurological Institute (MNI) standard brain space using SPM12. Gray matter (GM), white matter (WM), and cerebrospinal fluid (CSF) segmentation maps were generated during the same normalization process. The following steps were used for processing resting-state fMRI (rsfMRI) images. 1) The first 6 rsfMRI volumes of each subject were discarded from each subject's resting-state fMRI data to allow image intensity to reach steady state; 2) The remaining images were corrected for slice timing acquisition difference using the middle slice as the reference and then corrected for head motions using the first image volume as the reference. All subjects included in the following analyses had no more than 2 mm translational motions and no more than 2 degrees of angular motions; 3) rsfMRI images were spatially co-registered with the high definition structural MRI. WM and CSF segmentation maps were back-registered into the rsfMRI image space and resampled to have the same image resolution to be used as masks for extracting the mean WM and CSF signals; 4) temporal nuisance correction was performed via simple regression by including head motion timecourses, WM signal, and CSF signal as nuisance; Global signal regression was not used (Saad et al. 2012); 5) rsfMRI images were warped into the MNI space using the special transform estimated from the structural MRI as mentioned above, and resampled with a resolution of $3 \times 3 \times 3 \text{ mm}^3$; 6) special smoothing was done with an isotropic Gaussian kernel with a full-width-at-half-maximum (FWHM) of 6 mm.

BEN mapping calculation

BEN was calculated using BENTbx (Wang et al. 2014) (<https://cfn.upenn.edu/~zewang/software.html>) after image pre-processing. BEN was calculated at each voxel Sample Entropy (SampEn) (Lake et al. 2002).

SampEn is an approximate entropy measure, which measures the temporal coherence of a time series through calculating the “logarithmic likelihood” that a small section (within a window of a length ‘m’) of the data “matches” with other sections will still “match” the others if the section window length increases by 1. “match” is defined by a threshold $< r$ times standard deviation of the entire time series. The window length was set to 3 and the cut off threshold was set to 0.6 (Wang et al. 2014). More details of BEN calculation can be found in the original BENTbx paper (Wang et al. 2014). The collection of all voxels' entropy values formed the BEN map, which was smoothed with an isotropic Gaussian kernel (FWHM = 6 mm) to suppress the structural brain difference between individuals which may not be accurately aligned during spatial normalization of each brain into the MNI space.

CBF calculation

The CBF maps were calculated with the commercial software on the GE AW workstation. To correct the partial volume effects (PVEs) introduced by the large voxel size used in ASL MRI, each individual subject's structural image was segmented into GM, VM, and CSF using SPM12. The corresponding GM, WM, and CSF probability maps were registered into the native ASL MRI space and subsampled to have the same spatial resolution as that of the raw ASL MRI. The PET-based method was then used to correct PVEs (Hu et al. 2010). PVEs-corrected CBF maps were finally warped into the MNI space using the spatial transform determined from the structural MRI.

fALFF calculation

fALFF was calculated at each voxel of the preprocessed rsfMRI. The time series of each voxel was transformed into the frequency domain through Fourier transform. The sum of the magnitude of the spectrum between 0.01–0.08 Hz was divided by the sum of the entire acquired frequency band, i.e., 0–0.25 Hz to get the so-called fALFF.

Statistical analysis

The voxel-wise BEN-CBF, BEN-fALFF, and CBF-fALFF associations were assessed with Pearson correlation analyses including all subjects. Additional analyses were performed for females and males separately to examine any potential sex effects. The association maps were thresholded based on the correlation coefficient r rather than the probability because a statistically

significant correlation may not necessarily be a strong correlation. Since a $|r| < 0.3$ is generally considered a weak correlation, the threshold of $|r| \geq 0.3$ was used, which actually corresponded to a p value < 0.05 for all correlation analyses performed in this study ($p \leq 0.0017, 0.0221, 0.0362$ for the entire group, the female group, and males, respectively). A cluster size > 100 was used to remove small suprathreshold clusters. The traditional multiple comparison correction was not performed here because the dependent and independent variables of the association analyses at one voxel are different from those of another voxel, resulting in a different scenario of multiple comparison than that in the traditional massive voxel-wise imaging behavior correlation analysis where each voxel is referred to the same regressor. While it is not clear for how to adapt the conventional multiple comparison correction for these voxel-wise between-modality analyses, we used a cluster size of > 100 voxels to remove the sporadic suprathreshold voxels.

To statistically assess the sex difference of the BEN-CBF, BEN-fALFF, CBF-fALFF correlations, the correlation maps obtained in each gender were converted into Z-maps based on Fisher's Z-transform according to Eq. (1) and Eq. (2) (Fisher 1921). A z-statistic variable was computed based on the difference of the transformed maps as Z maps (Potthoff 1966).

$$r' = \frac{1}{2} \log_e \left[\frac{1+r}{1-r} \right] \quad (1)$$

$$Z = \frac{r'_1 - r'_2}{\sqrt{\frac{1}{n_1 - 3} + \frac{1}{n_2 - 3}}} \quad (2)$$

The significance level was defined by $Z > 1.96$ (corresponding to $p < 0.05$), a cluster size > 100 was used to remove small suprathreshold clusters.

BEN, CBF, fALFF difference between females and males were examined by two-sample t-test, and the

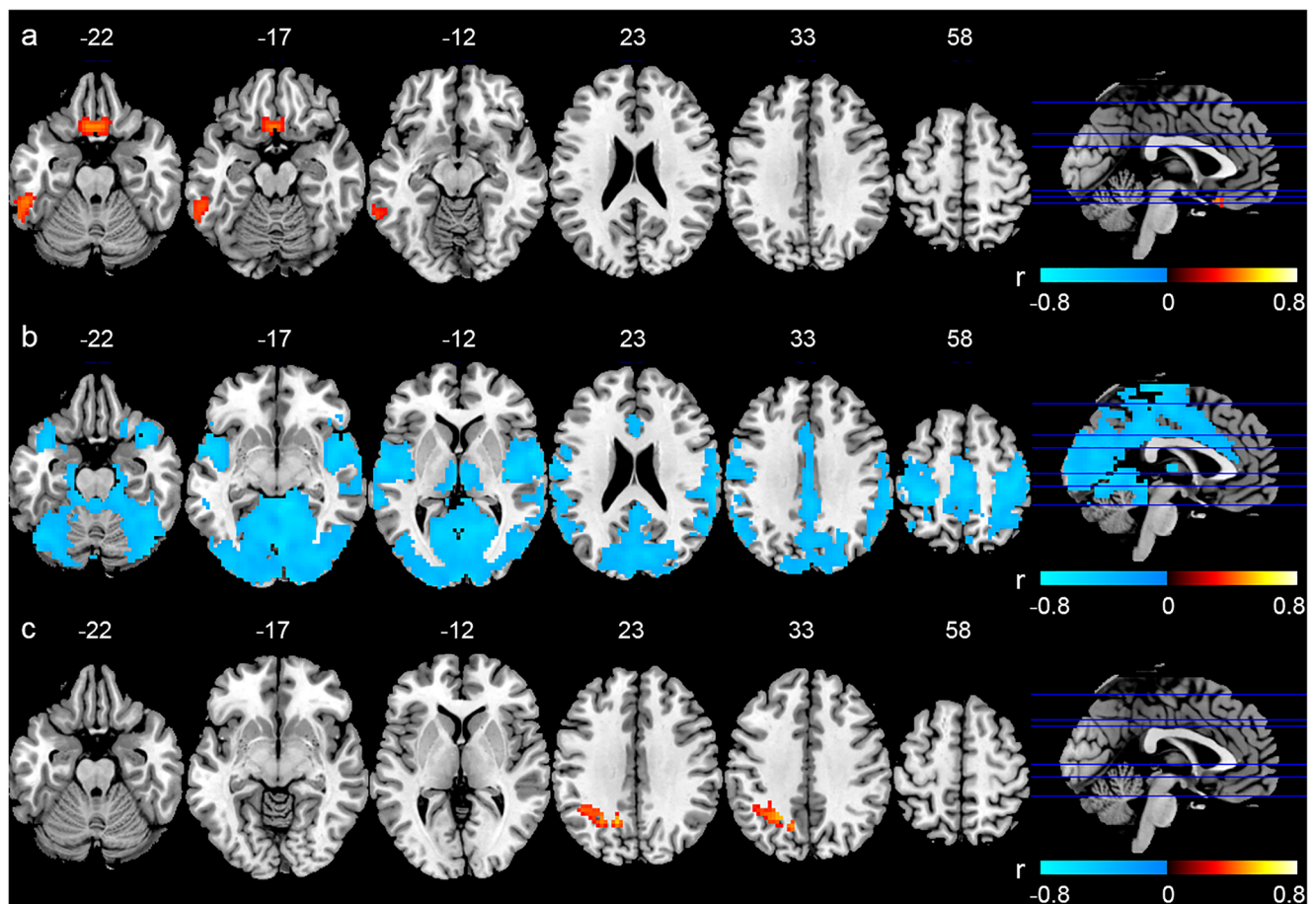


Fig. 1 Association maps (the Pearson correlation coefficient maps) of **a)** BEN-CBF, **b)** BEN-fALFF, **c)** CBF-fALFF. Hot color means positive correlation; cool color means negative correlation. Colorbars indicate the display window for the thresholded correlation coefficient maps.

The number above each slice indicates the slice location along the z-axis in the MNI space as also marked by the blue lines overlaid on the sagittal slice on the right

significance level was defined by a voxel-wise $p < 0.001$ and cluster size > 56 (corrected with AlphaSim, a Monte Carlo permutation based multiple-comparison correction tool provided by AFNI (<https://afni.nimh.nih.gov/>)).

Results

Positive BEN-CBF correlations were found in the medial orbitofrontal cortex (MOFC), left inferior temporal cortex (LITC) (Fig. 1a). Negative BEN-fALFF correlations were identified in temporal pole, insula, thalamus, superior temporal gyrus (STG), precentral gyrus, postcentral gyrus, supplementary motor area (SMA), precuneus, visual cortex (VC), fusiform, and lingual gyrus (Fig. 1b). Figure 1c shows the results of CBF-fALFF association analysis. Only positive CBF-fALFF correlations were found in several regions including left angular gyrus, and left precuneus.

Figure 2 shows the sex effects revealed by two-sample t-test. Both BEN (Fig. 2a) and fALFF (Fig. 2c) showed no significant sex difference ($p < 0.001$, cluster size > 56). CBF was significantly higher in females than males (Fig. 2b).

Figure 3 shows the BEN-CBF association analysis results for each gender. Females had BEN-CBF correlations in fewer brain regions including thalamus, middle temporal gyrus (MTG), (Fig. 3a). By contrast, males showed BEN-CBF correlations in more distributed areas including MPFC, bilateral OFC, superior temporal cortex, insula, and right VC (Fig. 3b). Females showed more positive BEN-CBF correlation in thalamus, while males had more positive BEN-CBF correlation in insula, postcentral cortex.

Figure 4 is the results of BEN-fALFF association analysis for each gender. Female showed negative BEN-fALFF correlations in more extended brain regions covering the DMN, VC, motor cortex, and anterior temporal lobe than males.

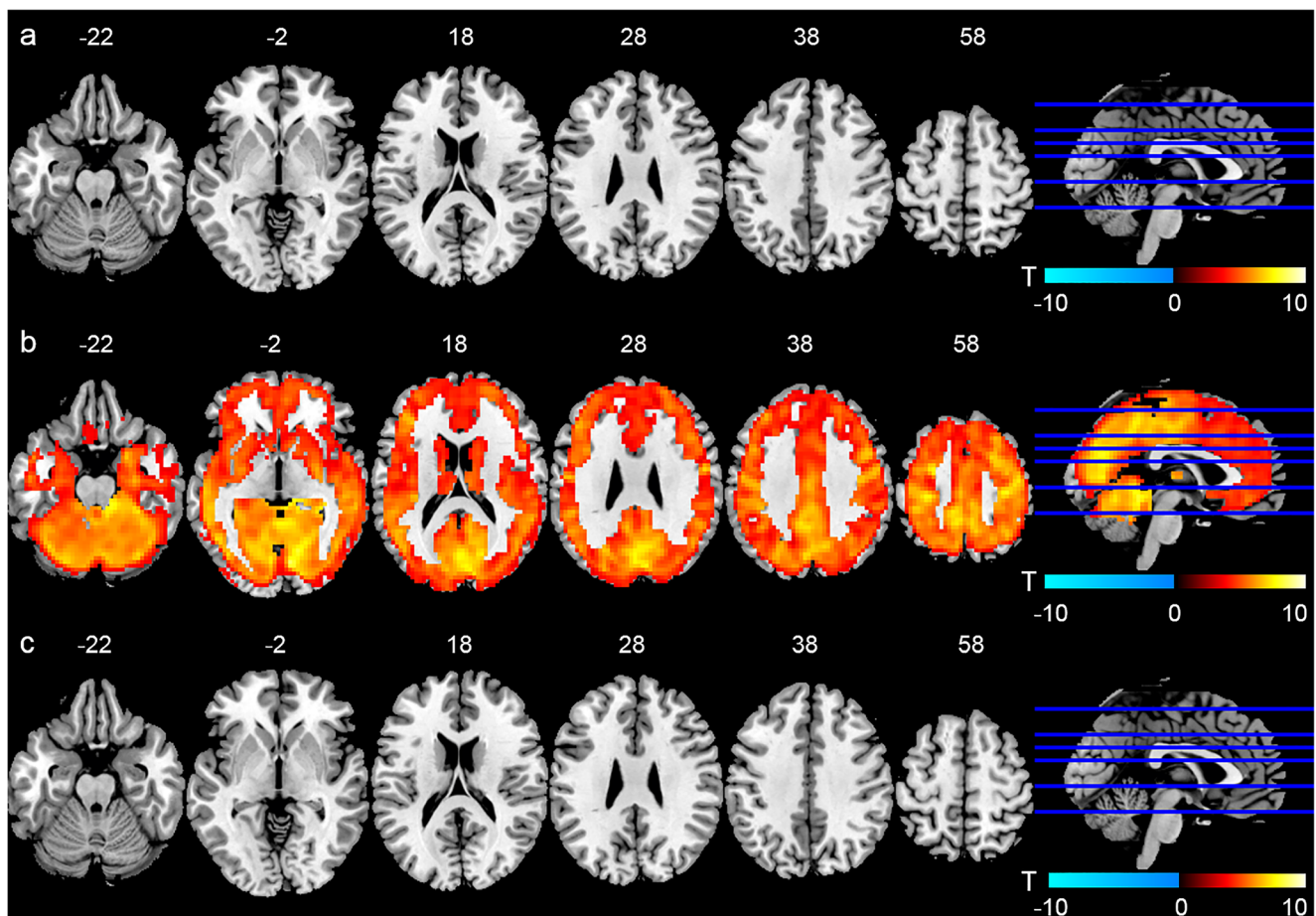


Fig. 2 Sex difference (T-value of the two-sample t-test) of **a)** BEN, **b)** CBF and **c)** fALFF. Hot color means greater in female; cool color means greater in male. Colorbars indicate the display window for the thresholded

T-value maps. The number above each slice indicates the slice location along the z-axis in the MNI space as also marked by the blue lines overlaid on the sagittal slice on the right

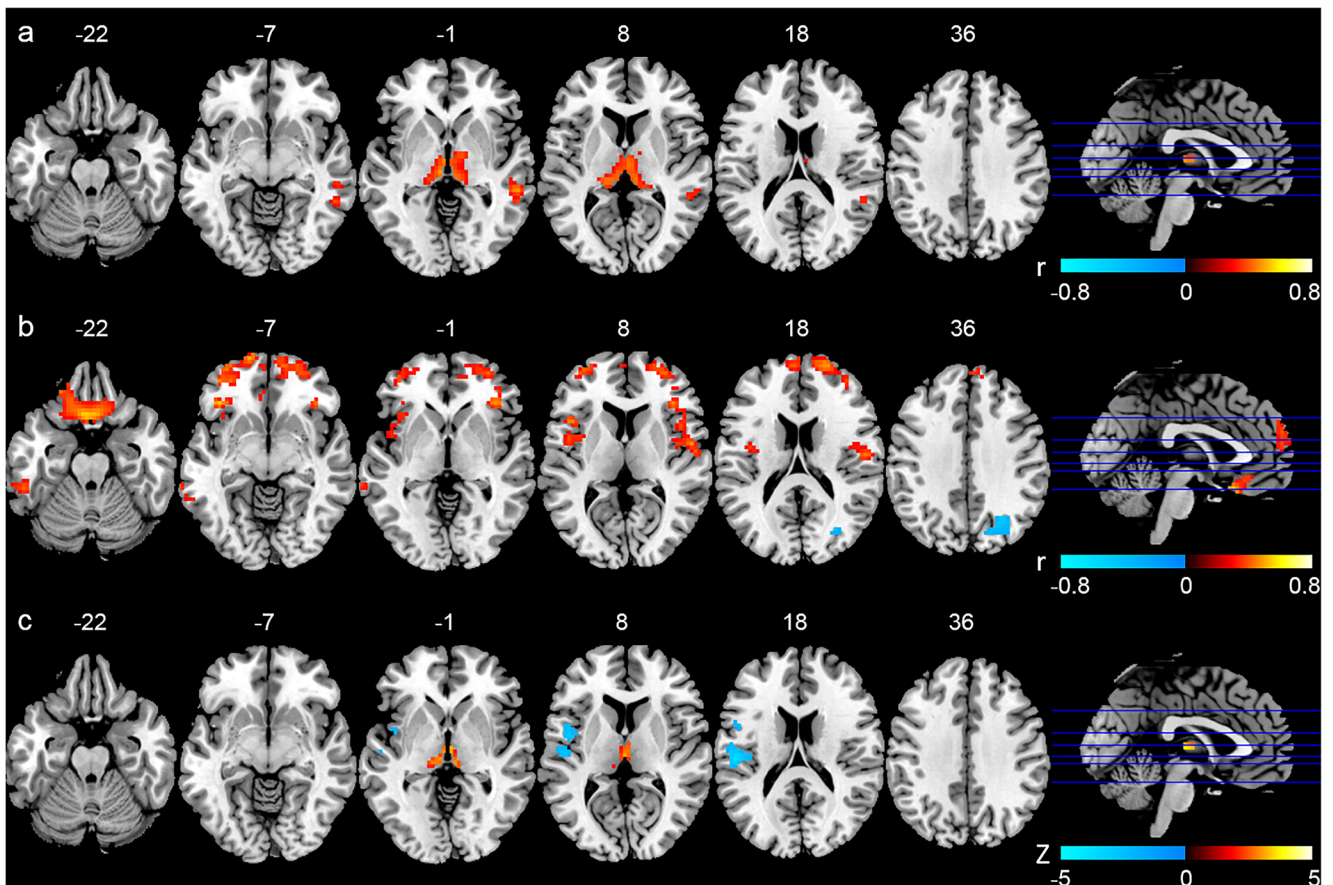


Fig. 3 BEN-CBF associations identified in **a)** the females, **b)** males, **c)** difference of females and males. For the first two rows, hot color means positive correlation; cool color means negative correlation. For the bottom row, hot and cool color mean that female had higher and lower

BEN-CBF correlations, respectively. Colorbars indicate the display window for the thresholded correlation coefficient maps. The number above each slice indicates the slice location along the z-axis in the MNI space as also marked by the blue lines overlaid on the sagittal slice on the right

Figure 5 shows the sex effects of CBF-fALFF associations. Males presented positive CBF-fALFF association in more cortical and subcortical areas than females.

Discussions

As a relatively new brain activity measure, BEN has gained more and more research attentions. But its neuronal basis still remains unclear though neurobiological studies had shown the association of entropy to neuronal adaptation at the cellular level (Adibi et al. 2013). Without neuronal level data, one alternative approach is to examine the correlations of BEN to other brain activity measures that are more established regarding their neuronal underpinnings. Such association analyses can also reveal how much different information can BEN provide to assess brain activity as compared to the more established measures. In this paper, a comprehensive study was performed to identify the potential associations between BEN and CBF, as well as fALFF. Our

data showed that BEN is correlated to baseline CBF only in a small portion of brain cortex including MOFC, LOFC, and left ITC. BEN was mainly inversely related to fALFF in a large portion of the brain, including cerebellum, VC, temporal cortex, motor cortex, and precuneus. Between fALFF and CBF, positive correlations were found in MOFC, LOFC, DLPFC, and parietal cortex, which are part of the default mode network (DMN) (Raichle et al. 2001). These between modality correlations were found to differ across sexes.

As BEN measures the phasic (dynamic) property of brain activity, while baseline CBF indicates the average brain activity, the spatially restricted BEN-CBF correlations suggest a disassociation between the phasic (dynamic) and tonic (baseline or on average) brain activity in most part of the brain, where BEN and CBF provide independent information about brain activity in most of the brain. The decoupling of BEN to baseline energy spend (as reflected by CBF) may reflect the capability our brain to achieve maximum information processing functionality under the constraint of total

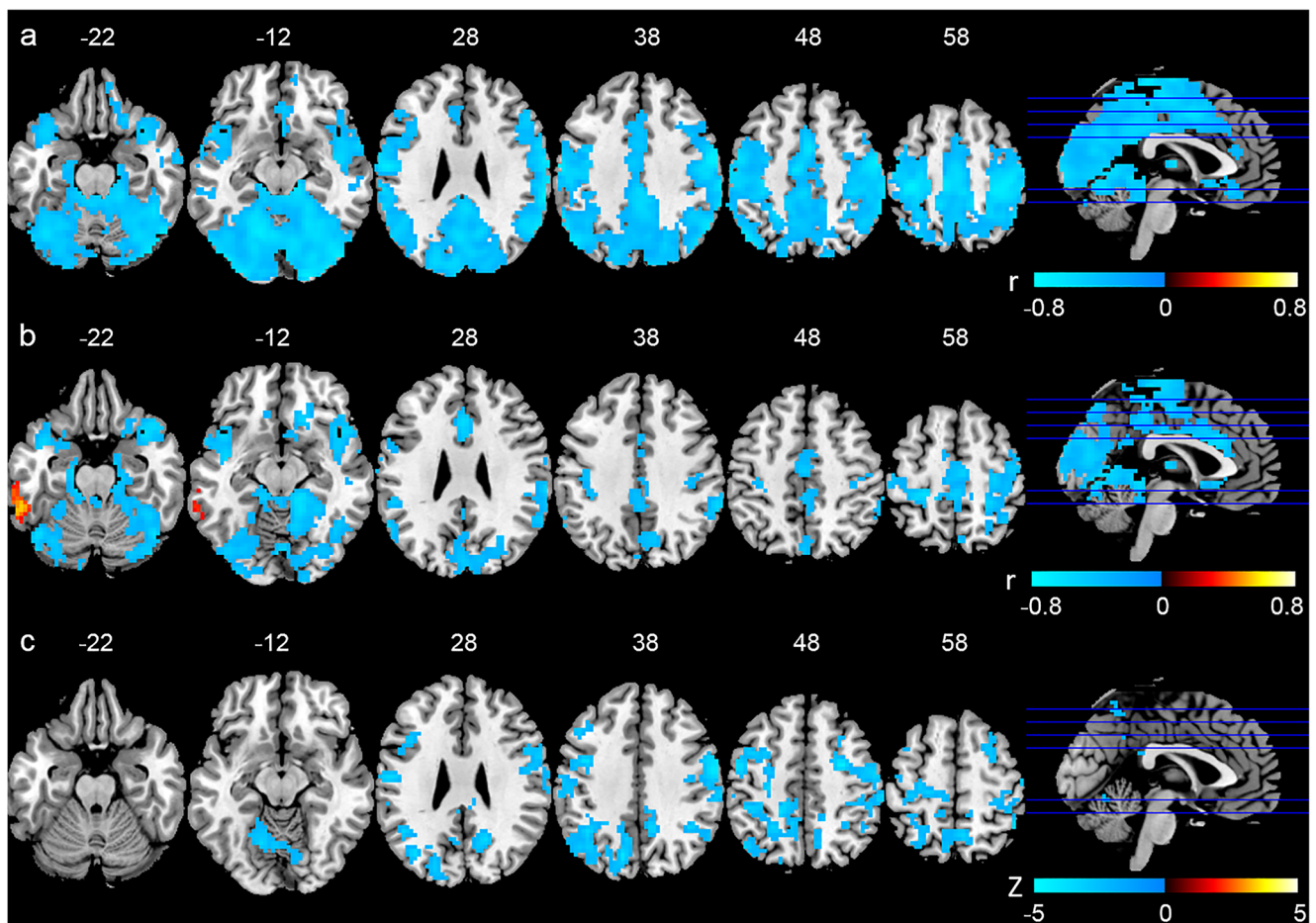


Fig. 4 BEN-fALFF associations (Pearson correlation coefficient) found in **a**) the females, **b**) males, **c**) difference of females and males. For the first two rows, hot color means positive correlation; cool color means negative correlation. For the bottom row, hot and cool color mean that female had higher and lower BEN-fALFF correlations, respectively.

Colorbars indicate the display window for the thresholded correlation coefficient maps. The number above each slice indicates the slice location along the z-axis in the MNI space as also marked by the blue lines overlaid on the sagittal slice on the right

available energy supply. Limited BEN-CBF associations were observed in anterior PFC, OFC, and ITC. OFC and anterior PFC receives intense projections from thalamus and midbrain areas (Fuster 2015), indicating a high volume of information processing. OFC and anterior PFC are part of the DMN with high resting brain activity and CBF. The positive BEN-CBF correlations found therein suggest that part of that energy spend is to facilitate the high information processing and so BEN in those regions.

fALFF is a widely adopted metric for resting state brain activity, which is empirically defined as the proportion of the low-frequency components in relative to the entire signal spectrum. By contrast, entropy has a statistical origin and is derived from the distribution of the underlying signal, which doesn't depend on a specific frequency band. Theoretically, BEN and fALFF are not necessarily related to each other. In this study, we found that BEN was negatively related to fALFF in VC, motor cortex, precuneus, and temporal cortex. These

regions have been well known to have elevated low-frequency brain activity fluctuations during resting state (Biswal et al. 1995, Lowe et al. 1998, Kiviniemi et al. 2000, Greicius et al. 2003). The increased low-frequency resting brain activity consequently reduces the overall irregularity of resting state brain activity as we observed in previous paper (Wang et al. 2014) and induces a negative BEN-fALFF correlation. The lack of BEN-fALFF correlation in most of brain suggests that BEN and fALFF are mutually independent in a large portion of the brain. As BEN is independent of a specific frequency band, assessing BEN may provide more comprehensive picture of brain activity especially in those regions without BEN-fALFF associations.

Positive CBF-fALFF correlations were found in a small portion of the DMN, including MOFC, MPFC, left angular gyrus, and left precuneus, which was supported by our previous CBF-ALFF association study (Li et al. 2012). The association pattern extension difference (we found CBF-ALFF correlation in most of brain cortex) can be explained by the

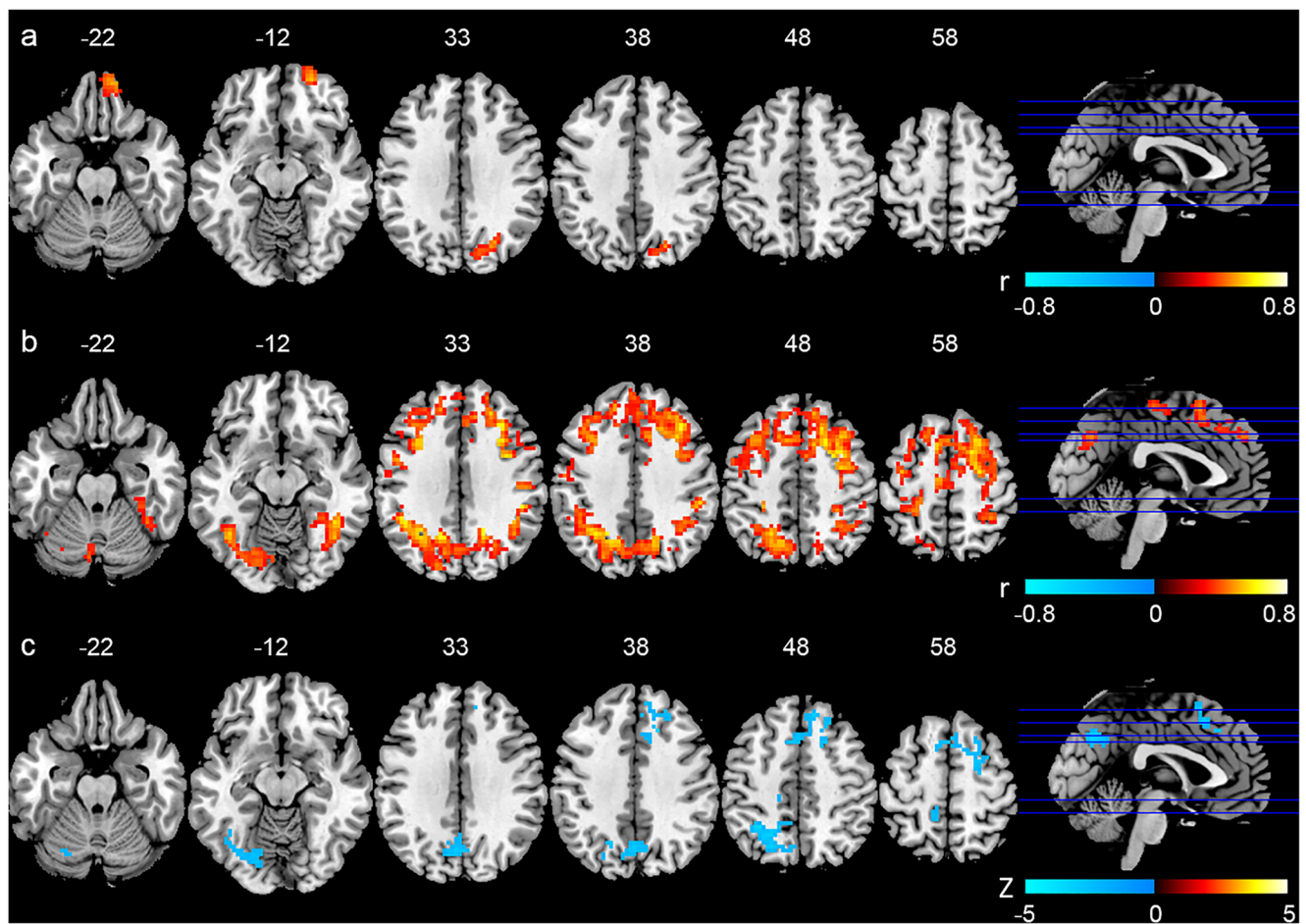


Fig. 5 CBF-fALFF associations (Pearson correlation coefficient) found in **a)** the females, **b)** males, **c)** difference of females and males. For the first two rows, hot color means positive correlation; cool color means negative correlation. For the bottom row, hot and cool color mean that female had higher and lower CBF-fALFF correlations, respectively.

difference between ALFF and fALFF: ALFF is the magnitude of the low-frequency bold signal which may be more affected by CBF than fALFF which is a scale-free number if we recall that BOLD signal is mainly contributed by CBF (Zou et al. 2008), and sample size (Zou et al. 2015).

Significant sex difference was found in CBF, which is well known in the literature (Rodriguez et al. 1988, Gur and Gur 1990). No sex difference was found in BEN and fALFF. Regarding the sex effects on the between-modality associations, BEN-CBF correlations were located in the thalamus, putamen, and temporal cortex in women but were shifted toward anterior part of the brain in men. As females had higher baseline CBF, there is much big room for the brain to fuse more energy without increasing CBF to facilitate an increase of BEN. By contrast, men's brain would need an increase of CBF to achieve a better information processing (BEN) in OFC, PFC, insula, and temporal cortex. Women and men showed similar BEN-fALFF association pattern with difference in terms of the association

Colorbars indicate the display window for the thresholded correlation coefficient maps. The number above each slice indicates the slice location along the z-axis in the MNI space as also marked by the blue lines overlaid on the sagittal slice on the right

cluster size. Male had more widespread CBF-fALFF association across the cortex. These gender difference can be similarly explained by the CBF gender difference as discussed above. Females have higher CBF, providing bigger room to meet the energy demand of resting state brain activity without further increasing CBF. Although more information will be required to fully understand these sex differences, they certainly raise a need to consider gender as an important fact when study brain activity.

In summary, we used a large cohort of healthy subjects to show that BEN, an emerging brain activity measure, only correlates to two widely used metrics: CBF and fALFF in a small part of brain. Our data demonstrate that BEN, CBF, and fALFF are complimentary brain function measures with very limited overlap; gender plays a role in BEN and CBF and their correlations to each other.

Funding This study was funded by Natural Science Foundation of Zhejiang Province (Grant LZ15H180001), the Youth 1000 Talent

Program of China, and Hangzhou Qianjiang Endowed Professor Program, National Natural Science Foundation of China (No. 61671198).

Compliance with ethical standards

Conflict of interest All authors declared no conflict of interest.

Ethical approval All procedures performed in studies involving human participants were in accordance with the ethical standards of the institutional and national research committee and with the 1964 Helsinki declaration and its later amendments or comparable ethical standards. This article does not contain any studies with animals performed by any of the authors.

Informed consent Informed written consents were obtained from all individual participants included in the study.

References

- Adibi, M., Clifford, C. W., & Arabzadeh, E. (2013). Informational basis of sensory adaptation: Entropy and single-spike efficiency in rat barrel cortex. *Journal of Neuroscience the Official Journal of the Society for Neuroscience*, 33(37), 14921–14926.
- Baron, J. C., Lebrun-Grandie, P., Collard, P., Cruzel, C., Mestelan, G., & Bousser, M. G. (1982). Noninvasive measurement of blood flow, oxygen consumption, and glucose utilization in the same brain regions in man by positron emission tomography: Concise communication. *Journal of Nuclear Medicine*, 23(5), 391–399.
- Bassett, D. S., & Gazzaniga, M. S. (2011). Understanding complexity in the human brain. *Trends in Cognitive Sciences*, 15(5), 200.
- Bhattacharya, J. (2000). Complexity analysis of spontaneous EEG. *Acta Neurobiologiae Experimentalis*, 60(4), 495.
- Biswal, B., Zerrin Yetkin, F., Haughton, V. M., & Hyde, J. S. (1995). Functional connectivity in the motor cortex of resting human brain using echo-planar mri. *Magnetic Resonance in Medicine*, 34(4), 537–541.
- Bosl, W., Tierney, A., Tager-Flusberg, H., & Nelson, C. (2011). EEG complexity as a biomarker for autism spectrum disorder risk. *BMC Medicine*, 9(1), 18.
- Clausius, R. (1862). Ueber die wärmeleitung gasförmiger körper. *Annalen der Physik*, 191(1), 1–56.
- Da, C., Song, D., Jian, Z., Shang, Y., Qiu, G., & Wang, Z. (2018). Caffeine caused a widespread increase of resting brain entropy. *Scientific Reports*, 8(1), 2700.
- DeWitt, D. S., Yuan, X. Q., Becker, D. P., & Hayes, R. L. (1988). Simultaneous, quantitative measurement of local blood flow and glucose utilization in tissue samples in normal and injured feline brain. *Brain Injury*, 2(4), 291–303.
- Fisher, R. A. (1921). On the “probable error” of a coefficient of correlation. *Metron*, 1, 1–32.
- Fransson, P. (2005). Spontaneous low-frequency BOLD signal fluctuations: An fMRI investigation of the resting-state default mode of brain function hypothesis. *Human Brain Mapping*, 26(1), 15–29.
- Friston, K. J., Frith, C. D., Passingham, R. E., Dolan, R. J., Liddle, P. F., & Frackowiak, R. S. (1992). Entropy and cortical activity: Information theory and PET findings. *Cerebral Cortex*, 2(3), 259–267.
- Friston, K. J., Tononi, G., Sporns, O., & Edelman, G. M. (2010). Characterising the complexity of neuronal interactions. *Human Brain Mapping*, 3(4), 302–314.
- Furlow Jr., T. W., Martin, R. M., & Harrison, L. E. (1983). Simultaneous measurement of local glucose utilization and blood flow in the rat brain: An autoradiographic method using two tracers labeled with carbon-14. *Journal of Cerebral Blood Flow and Metabolism*, 3(1), 62–66.
- Fuster, J. (2015). The prefrontal cortex (Fifth Edition). Elsevier Ltd.
- Goldberger, A. L., Peng, C. K., & Lipsitz, L. A. (2002). What is physiologic complexity and how does it change with aging and disease? *Neurobiology of Aging*, 23(1), 23–26.
- Greicius, M. D., Krasnow, B., Reiss, A. L., & Menon, V. (2003). Functional connectivity in the resting brain: A network analysis of the default mode hypothesis. *Proceedings of the National Academy of Sciences of the United States of America*, 100(1), 253–258.
- Gur, R. E., & Gur, R. C. (1990). Gender differences in regional cerebral blood flow. *Schizophrenia Bulletin*, 16(2), 247–254.
- Hofman, M. A. (2014). Evolution of the human brain: When bigger is better. *Frontiers in Neuroanatomy*, 8, 15.
- Hu, W. T., Wang, Z., Lee, V. M. Y., Trojanowski, J. Q., Detre, J. A., & Grossman, M. (2010). Distinct cerebral perfusion patterns in FTL and AD. *Neurology*, 75(10), 881–888.
- Jia, Y., Gu, H., & Luo, Q. (2017). Sample entropy reveals an age-related reduction in the complexity of dynamic brain. *Scientific Reports*, 7(1), 7990.
- Kiviniemi, V., Jauhainen, J., Tervonen, O., Pääkkö, E., Oikarinen, J., Vainionpää, V., Rantala, H., & Biswal, B. (2000). Slow vasomotor fluctuation in fMRI of anesthetized child brain. *Magnetic Resonance in Medicine*, 44(3), 373.
- Lake, D. E., Richman, J. S., Griffin, M. P., & Moorman, J. R. (2002). Sample entropy analysis of neonatal heart rate variability. *American Journal of Physiology Regulatory Integrative & Comparative Physiology*, 283(3), R789.
- Lebedev, A. V., Kaelin, M., Lövdén, M., Nilsson, J., Feilding, A., Nutt, D. J., & Carhart-Harris, R. L. (2016). LSD-induced entropic brain activity predicts subsequent personality change. *Human Brain Mapping*, 37(9), 3203.
- Lee, M. H., Smyser, C. D., & Shimony, J. S. (2013). Resting state fMRI: A review of methods and clinical applications. *Ajnr American Journal of Neuroradiology*, 34(10), 1866–1872.
- Li, Z., Zhu, Y., Childress, A. R., Detre, J. A., & Wang, Z. (2012). Relations between BOLD fMRI-derived resting brain activity and cerebral blood flow. *PLoS One*, 7(9), e44556.
- Li, Z., Fang, Z., Hager, N., Rao, H., & Wang, Z. (2016). Hyper-resting brain entropy within chronic smokers and its moderation by sex. *Scientific Reports*, 6, 29435.
- Lipsitz, L. A. (2004). Physiological complexity, aging, and the path to frailty. *Science of Aging Knowledge Environment Sage Ke*, 2004(16), pe16.
- Liu, Z. M., Schmidt, K. F., Sicard, K. M., & Duong, T. Q. (2004). Imaging oxygen consumption in forepaw somatosensory stimulation in rats under isoflurane anesthesia. *Magnetic Resonance in Medicine*, 52(2), 277–285.
- Lowe, M. J., Mock, B. J., & Sorenson, J. A. (1998). Functional connectivity in single and multislice echoplanar imaging using resting-state fluctuations. *NeuroImage*, 7(2), 119.
- Macphail, E. M., & Bolhuis, J. J. (2001). The evolution of intelligence: Adaptive specializations versus general process. *Biological Reviews of the Cambridge Philosophical Society*, 76(3), 341–364.
- Mölle, M., Marshall, L., Lutzenberger, W., Pietrowsky, R., Fehm, H. L., & Born, J. (1996). Enhanced dynamic complexity in the human EEG during creative thinking. *Neuroscience Letters*, 208(1), 61–64.
- Nelson, M. J., S. Dehaene, C. Pallier and J. T. Hale (2017). Entropy reduction correlates with temporal lobe activity. The Workshop on Cognitive Modeling & Computational Linguistics.
- Pothoff, R. F. (1966). Statistical aspects of problem of biases in psychological tests. North Carolina State University. Department of Statistics.
- Raichle, M. E. (1998). Behind the scenes of functional brain imaging: A historical and physiological perspective. *Proceedings of the*

- National Academy of Sciences of the United States of America*, 95(3), 765–772.
- Raichle, M. E., MacLeod, A. M., Snyder, A. Z., Powers, W. J., Gusnard, D. A., & Shulman, G. L. (2001). A default mode of brain function. *PNAS*, 98, 676–682.
- Richman, J. S., & Moorman, J. R. (2000). Physiological time-series analysis using approximate entropy and sample entropy. *American Journal of Physiology Heart & Circulatory Physiology*, 278(6), H2039.
- Rilling, J. K. (2014). Comparative primate neuroimaging: Insights into human brain evolution. *Trends in Cognitive Sciences*, 18(1), 46–55.
- Rodriguez, G., Warkentin, S., Risberg, J., & Rosadini, G. (1988). Sex differences in regional cerebral blood flow. *Journal of Cerebral Blood Flow and Metabolism*, 8(6), 783–789.
- Roth, G., & Dicke, U. (2012). Evolution of the brain and intelligence in primates. *Progress in Brain Research*, 195, 413–430.
- Saad, Z. S., Gotts, S. J., Murphy, K., Chen, G., Jo, H. J., Martin, A., & Cox, R. W. (2012). Trouble at rest: How correlation patterns and group differences become distorted after global signal regression. *Brain Connectivity*, 2(1), 25.
- Sabeti, M., Katebi, S., & Boostani, R. (2009). Entropy and complexity measures for EEG signal classification of schizophrenic and control participants. *Artificial Intelligence in Medicine*, 47(3), 263–274.
- Shannon, C. E. (1948). A mathematical theory of communication. *Bell System Technical Journal*, 27, 379–423–623–656.
- Singer, W. (2009). The brain, a complex self-organizing system. *European Review*, 17(2), 321–329.
- Smith, R. X., Yan, L., & Wang, D. J. J. (2014). Multiple time scale complexity analysis of resting state FMRI. *Brain Imaging & Behavior*, 8(2), 284.
- Sokunbi, M., Fung, W., Sawlani, V., Choppin, S., Linden, D., & Thome, J. (2014a). Resting state fMRI entropy probes complexity of brain activity in adults with ADHD. *Psychiatry Research: Neuroimaging*, 214(3), 341–348.
- Sokunbi, M. O., Gradin, V. B., Waiter, G. D., Cameron, G. G., Ahearn, T. S., Murray, A. D., Steele, D. J., & R. T. Staff. (2014b). Nonlinear complexity analysis of brain FMRI signals in schizophrenia. *PLoS One*, 9(5), e95146.
- Song, D., Chang, D., Zhang, J., Peng, W., Shang, Y., Gao X., & Wang, Z. (2018). Reduced brain entropy by repetitive transcranial magnetic stimulation on the left dorsolateral in the healthy young adults. *Brain Imaging & Behavior*, 1–9.
- Tononi, G., Edelman, G. M., & Sporns, O. (1998). Complexity and coherency: Integrating information in the brain. *Trends in Cognitive Sciences*, 2(12), 474–484.
- Vestergaard, M. B., Lindberg, U., Aachmann-Andersen, N. J., Lisbjerg, K., Christensen, S. J., Law, I., Rasmussen, P., Olsen, N. V., & Larsson, H. B. (2016). Acute hypoxia increases the cerebral metabolic rate - a magnetic resonance imaging study. *Journal of Cerebral Blood Flow and Metabolism*, 36(6), 1046–1058.
- Wang, Z., Li, Y., Childress, A. R., & Detre, J. A. (2014). Brain entropy mapping using fMRI. *PLoS One*, 9(3), e89948.
- Wang, B., Niu, Y., Miao, L., Cao, R., Yan, P., Guo, H., Li, D., Guo, Y., Yan, T., & Wu, J. (2017). Decreased complexity in Alzheimer's disease: Resting-state fMRI evidence of brain entropy mapping. *Frontiers in Aging Neuroscience*, 9, 378.
- Yang, A. C., Huang, C. C., Yeh, H. L., Liu, M. E., Hong, C. J., Tu, P. C., Chen, J. F., Huang, N. E., Peng, C. K., Lin, C. P., & Tsai, S. J. (2013). Complexity of spontaneous BOLD activity in default mode network is correlated with cognitive function in normal male elderly: A multiscale entropy analysis. *Neurobiology of Aging*, 34(2), 428–438.
- Yao, Y., Lu, W. L., Xu, B., Li, C. B., Lin, C. P., Waxman, D., & Feng, J. F. (2013). The increase of the functional entropy of the human brain with age. *Scientific Reports*, 3, 2853.
- Ze Wang, J. S., Duan, D., Damley, S., Jing, Y., Zhang, J., O'Brien, C., & Childress, A. R. (2017). A hypo-status in drug dependent brain revealed by multi-modal MRI. *Addiction Biology*, 22(6), 1622–1631.
- Zhou, F., Zhuang, Y., Gong, H., Zhan, J., Grossman, M., & Wang, Z. (2016). Resting state brain entropy alterations in relapsing remitting multiple sclerosis. *PLoS One*, 11(1), e0146080.
- Zou, Q. H., Zhu, C. Z., Yang, Y., Zuo, X. N., Long, X. Y., Cao, Q. J., Wang, Y. F., & Zang, Y. F. (2008). An improved approach to detection of amplitude of low-frequency fluctuation (ALFF) for resting-state fMRI: Fractional ALFF. *Journal of Neuroscience Methods*, 172(1), 137–141.
- Zou, Q., Wu, C. W., Stein, E. A., Zang, Y., & Yang, Y. (2009). Static and dynamic characteristics of cerebral blood flow during the resting state. *NeuroImage*, 48(3), 515–524.
- Zou, Q., Miao, X., Liu, D., Wang, D. J. J., Zhuo, Y., & Gao, J. H. (2015). Reliability comparison of spontaneous brain activities between BOLD and CBF contrasts in eyes-open and eyes-closed resting states. *Neuroimage*, 121, 91–105.